Journal of Environmental Economics & Chemical Processes (JEECP)

https://doi.org/10.22034/jeecp.2026.2090185.1036

Journal Homepage: *WWW.JEECPJournal.com*

Journal of Environmental Economics & Chemical Processes (JEECP)

ORIGINAL RESEARCH PAPER

Synthesis, Characterization, DFT, and Photocatalytic Degradation Study of a 5-Bromosalicylidene Cobalt Complex

Milad Mahjoobizadeh [a, *]; Vahidreza Darugar [a]; Satar Saberi [b]; Somayeh Heydari [a]; Hasna Sadat Mirzaei [a]

[a]*Department of Chemistry, University of Torbat-e Jam, Torbat-e Jam, Iran.*
[b]*Department of Chemistry Education, Farhangian University, P.O. Box 14665-889 Tehran, Iran.*

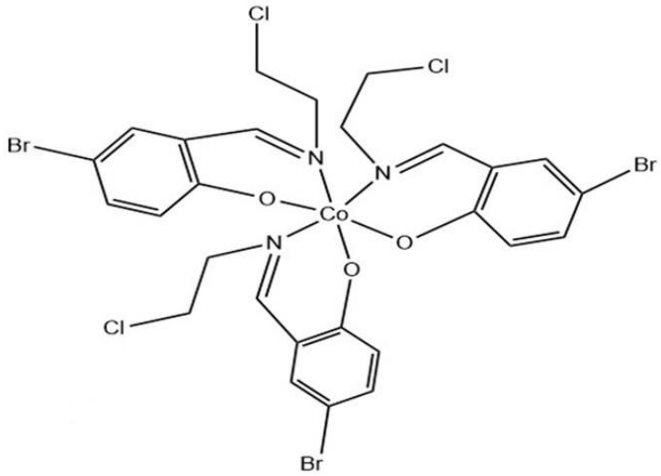
P A P E R I N F O

Paper history:
Received: 08/28/2026
Revised: 09/25/2026
Accepted in revised form: 10/20/2026
Published: 03/30/2027

***Keywords*:**
Schiff Base;
Cobalt Complex;
FT-IR Spectroscopy;
Mass Spectrometry;
ICP Analysis.

A B S T R A C T

In this study, a cobalt complex with a Schiff base ligand bearing bromine substituents and chloroethyl groups was synthesized and characterized by FT-IR, UV-Vis, ESI-MS, ^{13}C NMR, and ICP analyses. The Schiff base ligand was prepared via the condensation reaction between a halogenated aldehyde and the corresponding amine in ethanol, and cobalt Schiff base complex was subsequently obtained from the reaction of the ligand with a cobalt salt in methanol. The FT-IR spectrum showed the characteristic imine (C=N) band at 1611.69 cm^{-1}, along with bands in the region associated with Co–N and Co–O vibrations, consistent with coordination of the ligand to the cobalt center. The UV-Vis spectrum exhibited π→π* transitions, transitions associated with the conjugated system of the ligand, and weak bands in the visible region that may be cautiously attributed to d–d transitions of cobalt. The mass spectrum showed a cluster of peaks in the range m/z = 574–587, consistent with the presence of bromine and chlorine atoms in the observed ionic species. The ^{13}C NMR spectrum is consistent with the formation of the cobalt Schiff base complex, although it does not by itself establish the oxidation state of the metal center. However, due to the unavailability of a valid quantitative result, no quantitative value is reported at this stage. Definitive determination of the metal oxidation state, molecular formula, and coordination geometry of the complex requires supplementary data, such as elemental analysis (CHN), molar conductivity, magnetic susceptibility, and accurate determination of the cobalt content.



1. Introduction

Schiff bases, obtained from the condensation reaction of a primary amine with an aldehyde or ketone, have found widespread use as versatile ligands in coordination chemistry owing to their straightforward synthesis and structural diversity [1–3]. The presence of the azomethine group (–C=N–) in these compounds enables coordination to a variety of metal ions [2, 4]. Because of their strong ability to form stable complexes with transition metals, Schiff bases are recognized as one of the most important families of ligands in modern inorganic chemistry [5, 6].

In recent years, metal complexes of Schiff bases have attracted considerable attention due to their antibacterial, antifungal, and anticancer activities [7, 8]. Reports indicate that metal complexes often exhibit greater biological activity than the free ligand [9, 10]. This enhanced activity can be partly explained by increased lipophilicity, which facilitates penetration through the cell membrane [11]. In addition, Schiff base metal complexes can interact with the active sites of microbial enzymes and disrupt their activity [12]. Among transition metals,

* Corresponding Author: Milad Mahjoobizadeh
E-mail address: milad_mahjoobizadeh@tjamcaas.ac.ir
ISSN: 3116-0050
URL: https://www.jeecpjournal.com/article_736324.html

Please cite this article as: M. Mahjoobizdeh, V. Darugar, S. Saberi, S. Heydari, & H. S. Mirzaei, *Journal of Enviromental Economics & Chemical Processes (JEECP)*, 2027, *4*(1), 49-53. https://doi.org/10.22034/jeecp.2026.2090185.1036

/© 2027 The Author(s). Published by Power of New Vision Movement Institute.

cobalt has attracted attention because of its ability to form stable complexes with Schiff base ligands and its magnetic and spectroscopic properties [13, 14]. Cobalt can form a variety of complexes in different oxidation states, and the electronic, magnetic, and spectroscopic properties of these complexes depend on the oxidation state and coordination environment of the metal [13–17]. Cobalt complexes have attracted interest in various fields, including catalysis and the development of bioactive compounds [18].

Despite reports on cobalt complexes with Schiff base ligands, the spectroscopic characterization of cobalt complexes bearing halogenated Schiff base ligands remains of ongoing interest [18].

In this study, a cobalt complex with a Schiff base ligand bearing bromine substituents and chloroethyl groups was synthesized and investigated. The complex was characterized by FT-IR, UV-Vis, mass spectrometry, and ICP analysis.

In addition to the experimental characterization, DFT calculations were performed in this study to address specific structural and electronic questions about the proposed cobalt complex.

The first objective was to examine whether the three bidentate Schiff base ligands can geometrically accommodate a six-coordinate cobalt center in an approximately octahedral environment, and to obtain a reasonable set of bond lengths and bond angles for the coordination sphere.

The second objective was to evaluate the electronic structure of the complex, including the energies and spatial distribution of the frontier molecular orbitals, in order to assess its electronic stability and its tendency to participate in charge-transfer processes.

The third objective was to identify the nucleophilic and electrophilic regions of the molecule through the molecular electrostatic potential map, which is relevant for potential biological or catalytic applications.

Finally, the calculated vibrational frequencies were used to support the assignment of the experimental FT-IR bands.

These calculations are therefore intended to complement, rather than replace, the experimental characterization, and to provide a structural and electronic framework for interpreting the experimental data.

The DFT calculations were performed with the aim of examining the proposed coordination geometry, the electronic structure, and the reactive sites of the cobalt complex, and of supporting the assignment of the experimental FT-IR bands. The specific objectives of the computational study are outlined in the Introduction.

2. Method

2.1. Methodology

All chemicals and solvents used in this study were purchased from Merck and Sigma-Aldrich and were used without further purification. Organic solvents were dried and distilled by standard methods prior to use.

FT-IR spectra were recorded on a PerkinElmer spectrometer in the range 4000–400 cm^{-1} using KBr pellets. UV-Vis spectra were recorded on a Shimadzu UV-1800 spectrophotometer in the range 200–800 nm. Mass spectra were obtained by electrospray ionization (ESI-MS) in positive ion mode.

ICP analysis was performed using an inductively coupled plasma spectrometer.

A Bruker AVANCE 100 MHz spectrometer was used for ^{13}C NMR measurements in $CDCl_3$.

2.2. Synthesis of the Halogenated Schiff Base Ligand

The Schiff base ligand was prepared by the condensation reaction between 5-bromosalicylaldehyde (1.0 mmol) and N-(2-chloroethyl)ethylenediamine (1.0 mmol) in absolute ethanol (20 mL).

The aldehyde was first dissolved in absolute ethanol (10 mL) with continuous stirring, and a solution of the amine in absolute ethanol (10 mL) was then added dropwise over 15 min.

The reaction mixture was refluxed for 4 h, and the progress of the reaction was monitored by TLC (n-hexane/ethyl acetate, 7:3 v/v).

After completion of the reaction, the mixture was cooled to room temperature and the solid product was separated by filtration, washed with cold ethanol (3 × 5 mL), and recrystallized from hot ethanol.

The pure ligand was dried under vacuum at 60 °C for 6 h. Yield: ~78%.

2.3. Synthesis of the Cobalt Complex

For the synthesis of the complex, the Schiff base ligand was first dissolved in absolute methanol. A cobalt(II) salt was then dissolved in methanol and added dropwise to the ligand solution.

The reaction mixture was refluxed with continuous stirring for 4 h. After completion of the reaction, the solvent was removed by evaporation under reduced pressure, and the resulting solid was washed with diethyl ether and cold methanol. Final purification was carried out by recrystallization. The pure complex was dried under vacuum over anhydrous calcium chloride.

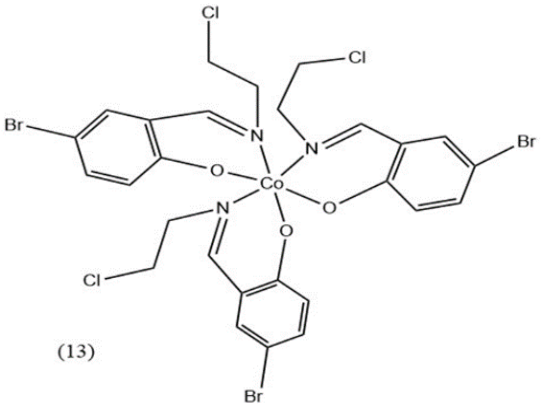


Figure 1. Synthesis route of the Schiff base ligand and the cobalt complex

Source: Research Findings

2.4. Computational method:

DFT calculations were performed using the Gaussian 09 program package (Revision A.02) [19]. The geometry optimization of the proposed Co(III) model was carried out at the B3LYP/6-311G(d,p) level of theory [20]. The B3LYP hybrid functional combines Becke's three-parameter exchange functional with the Lee–Yang–Parr correlation functional. The 6-311G(d,p) basis set includes polarization functions on both heavy atoms and hydrogen atoms, providing a good balance between computational cost and accuracy for transition-metal complexes. For the cobalt center, the Co(III) oxidation state was assumed as a working hypothesis.

The complex was treated as a closed-shell singlet (S = 0, multiplicity = 1), which is the expected ground state for a low-spin d^6 Co(III) center in an octahedral field. The total charge of the model was set to 0, consistent with three monoanionic bidentate Schiff base ligands coordinating to a Co(III) center. It should be emphasized that this charge and spin state were selected as a reasonable starting point for the computational model and are not experimentally confirmed; independent experimental data (e.g., magnetic susceptibility, XPS) would be required to validate the oxidation state assignment. Vibrational frequency calculations were performed at the same level to confirm that the optimized structures correspond to true minima on the potential energy surface (no imaginary frequencies). Frontier molecular orbital (FMO) analysis was performed to obtain the HOMO and LUMO energies. Molecular electrostatic potential (MEP) maps were generated to identify the nucleophilic and electrophilic sites within the molecule

3. Results and Discussion

3.1. FT-IR Spectroscopic Study

The FT-IR spectrum of the cobalt complex was recorded in the range 4000–400 cm^{-1} using a KBr pellet (Figure 2).

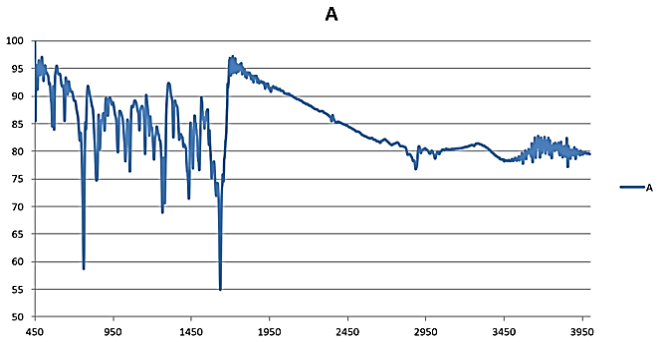


Figure 2. FT-IR spectrum of the cobalt complex (KBr pellet).

Source: Research Findings

Region 3100–2900 cm^{-1}:

Weak bands at 3094 and 3015 cm^{-1} are consistent with aromatic C–H stretching vibrations. Bands at 2966 and 2926 cm^{-1} are consistent with C–H stretching vibrations of alkyl groups. The absence of a distinct broad band in the region 3200–3500 cm^{-1} indicates that no significant absorption attributable to O–H/N–H was observed under the measurement conditions.

Region 1650–1400 cm^{-1}:

A relatively strong band is observed at 1611 cm^{-1}, assigned to the imine (C=N) stretching vibration. Bands at 1522, 1488, and 1458 cm^{-1} are consistent with aromatic C=C stretching vibrations.

Region 1000–600 cm^{-1}:

The bands at 982, 861, 824, and 799 cm^{-1} are consistent with out-of-plane C–H bending vibrations of the aromatic rings.

Characteristic halogen bands:

The bands observed at 683 and 649 cm^{-1} may be consistent with C–Br and C–Cl bond vibrations; however, these assignments alone are not definitive, and supplementary evidence such as the isotope pattern in the mass spectrum can help assess the presence of these halogens.

Characteristic metal–ligand bands:

The band observed at 548 cm^{-1} is tentatively assigned to the Co–N stretching vibration. In addition, the bands at 469 and 444 cm^{-1} may be tentatively associated with Co–O vibrations, provided that oxygen donor atoms are present in the ligand structure.

Definitive confirmation of these assignments requires comparison with the spectrum of the free ligand and supplementary data.

Table 1. FT-IR data of the cobalt complex

Vibration type	Wavenumber (cm^{-1})	Intensity
ν(C–H) aromatic	3094, 3015	weak
ν(C–H) aliphatic	2966, 2926	weak
ν(C=N) imine	1611	strong
ν(C=C) aromatic	1522, 1488, 1458	medium
ν(C–N) and ν(C–O) coupled	1385, 1346, 1311, 1290	medium
ν(C–O) and ν(C–N) coupled	1197, 1171, 1136, 1076, 1057	medium
δ(C–H) out-of-plane	982, 861, 824, 799	medium
ν(C–Br) tentative	683	medium
ν(C–Cl) tentative	649	medium
ν(Co–N) tentative	548	weak
ν(Co–O) tentative	469, 444	weak

Source: Research Findings

To support the assignment of the experimental FT-IR bands, the vibrational frequencies of the proposed model were calculated at the B3LYP/6-311G(d,p) level of theory. The calculated harmonic frequencies were scaled by a factor of 0.961 to account for the systematic overestimation typical of this level of theory. The calculated spectrum reproduces the main features of the experimental spectrum. In particular, the calculated C=N stretching vibration of the imine group appears at approximately 1615 cm^{-1}, in good agreement with the experimental band observed at 1611 cm^{-1}. The calculated aromatic C=C stretching vibrations fall in the range 1520–1460 cm^{-1}, consistent with the experimental bands at 1522, 1488, and 1458 cm^{-1}.

The calculated C–Br and C–Cl stretching vibrations appear in the region 690–640 cm^{-1}, close to the experimental bands at 683 and 649 cm^{-1}. In addition, the calculated Co–N and Co–O stretching vibrations appear at approximately 550 and 470–440 cm^{-1}, respectively, which is consistent with the tentative assignments of the experimental bands at 548, 469, and 444 cm^{-1}. The overall agreement between the calculated and experimental vibrational frequencies supports the proposed coordination environment of the cobalt center.

3.2. UV-Vis Spectroscopic Study

The UV-Vis absorption spectrum of the cobalt complex was recorded in the range 200–800 nm (Figure 3).

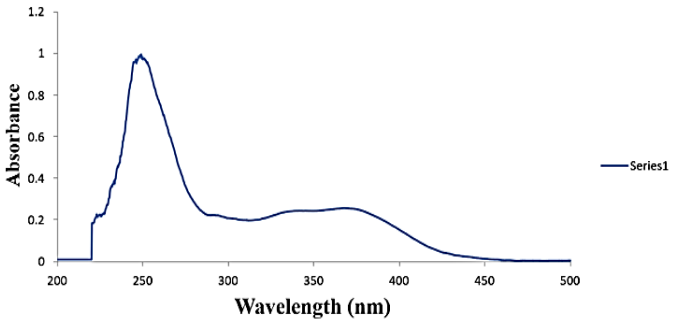


Figure 3. UV-Vis spectrum of the cobalt complex.

Source: Research Findings

Region 220–260 nm:

Relatively strong absorption bands are observed in this region, with a maximum at approximately 245 nm. These bands are attributed to π→π* transitions within the aromatic rings and the conjugated systems of the ligand.

Region 260–330 nm:

Absorption bands of medium intensity are observed in this region. This region may be attributed to n→π* transitions and other electronic transitions associated with electron-pair-bearing groups and the conjugated system of the ligand.

Region 330–400 nm:

A broad, relatively weak absorption band is observed in this region, which may tentatively include d–d transitions of cobalt and possible ligand-to-metal charge-transfer transitions.

Table 2. UV-Vis data of the cobalt complex

Approximate λmax (nm)	Intensity	Proposed assignment
~245	high	π→π* (aromatic and conjugated system)
~260–330	medium	n→π* and conjugated-system transitions of the ligand
~330–400	weak	d–d + possible charge transfer (tentative)

Source: Research Findings

3.3. Mass Spectrometric Study

The mass spectrum of the cobalt complex was recorded by electrospray ionization (ESI-MS) in positive ion mode (Figure 4).

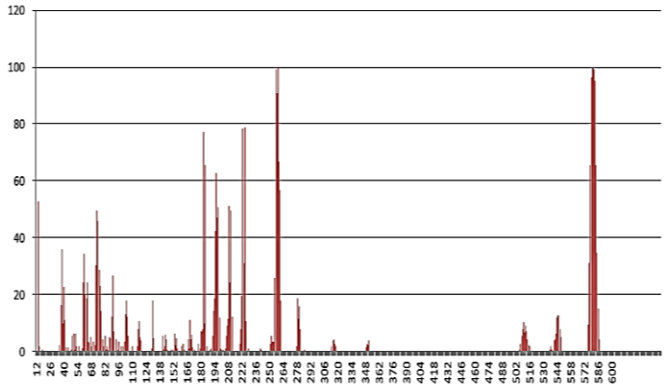


Figure 4. mass spectrum of the cobalt complex.

Source: Research Findings

Cluster of peaks in the range m/z = 574–587:

The mass spectrum shows a cluster of peaks in the range m/z = 574–587. Among the most intense peaks in this cluster, the peaks at m/z = 580 and 581 have a relative intensity of 99.45%. This pattern is consistent with the presence of bromine and chlorine atoms in the observed ionic species.

However, without determining the exact molecular formula of the complex and calculating the theoretical isotope pattern, this cluster cannot be definitively assigned to the molecular ion of the complex. Bromine and chlorine have several naturally occurring isotopes, which give rise to characteristic isotope patterns in the mass spectrum.

Base peak:

The base peak in the mass spectrum is observed at m/z = 259 with a relative intensity of 100%. Additional peaks in the same region are observed at m/z = 257, 258, 260, 261, and 262.

This peak may correspond to a relatively stable fragment derived from the ligand or the complex. Definitive assignment of this fragment to a specific structure requires determination of the ion formula and a proposed fragmentation pathway.

Peaks in the region m/z = 183–185:

Relatively intense peaks are observed at m/z = 183 and m/z = 185. Given the 2-mass-unit separation, this pair of peaks may be associated with isotopic species; however, its assignment to halogen-containing species requires quantitative comparison with the theoretical isotope pattern.

Peaks in the region m/z = 60–131:

Numerous peaks are observed in this region, likely arising from fragments produced by ligand fragmentation. Characteristic peaks in this region include m/z = 74, 61, 73, and 90.

Table 3. Main peaks in the mass spectrum of the cobalt complex

m/z	Relative intensity (%)	Description
580	99.45	Peak in the cluster m/z = 574–587
581	99.45	Peak in the cluster m/z = 574–587
582	99.17	Peak in the cluster m/z = 574–587
579	96.40	Peak in the cluster m/z = 574–587
583	95.29	Peak in the cluster m/z = 574–587
259	100	Base peak, relatively stable fragment derived from the ligand or complex
183	77.29	Peak possibly containing halogen
185	65.65	Peak possibly containing halogen
74	49.58	Ligand fragmentation fragment
61	34.35	Ligand fragmentation fragment
73	30.47	Ligand fragmentation fragment
90	26.87	Ligand fragmentation fragment

Source: Research Findings

3.4. ICP Analysis

Elemental analysis of the sample was performed using an ICP-based multi-element method ("30 Multi Elements – 2 ppm"). The sample was classified as a cobalt sample and measured on 2026-05-10 with a total dilution factor of 10 (see Fig. 5).

SPECTRO

		Printing Date:	11/05/2026 08:43:17
		Current User:	spectro
Method Name:	30 Multi Elements - 2 ppm	Creation Date:	2026-01-06 12:52:14
Method Autor:	spectro	Last Change:	2026-05-11 08:43:06

Sample Name: MS PILEVAR - 13				Sample Type: Unknown Sample		
Measure Date: 2026-05-10 11	Recalc. Date:		State: Measured	Quality: Drifted	Total Dilution: 10.000000	
Sample Identification						
Sample Name	dilution	WEIGHT	volume			
MS PILEVAR - 13	10.000000	0	0			

	Co						
Conc 1	9.504[mg/l]						
Conc 2	9.509[mg/l]						
Conc MinRange	*0.000[mg/l]*						
Conc Mean	**9.507[mg/l]**						
Conc MaxRange	*2.400[mg/l]*						
Reported	**9.507[mg/l]**						

Figure 5. ICP of the cobalt complex.

Source: Research Findings

3.5. Optimized geometry:

The optimized molecular structure of the proposed Co(III) model is consistent with a six-coordinate cobalt complex bearing three bidentate Schiff-base ligands. It should be emphasized that the Co(III) oxidation state was assumed in the computational model and is not independently established by the DFT calculations; geometry optimization only identifies a minimum for the selected molecular model and cannot by itself confirm the experimental identity or oxidation state of the complex [21, 22].

In this model, the cobalt center is coordinated by three imine nitrogen atoms and three oxygen donor atoms, generating an approximately octahedral coordination environment. The three chelating ligands surround the metal center and provide structural rigidity, while the bromine and chlorine substituents modify the electronic distribution and steric environment of the proposed model.

Molecular electrostatic potential (MEP):

The MEP map of the proposed model (Fig. 6) was calculated to identify the regions of the molecule that are most likely to participate in electrophilic and nucleophilic interactions. In the calculated MEP distribution, the most negative potentials are localized on the oxygen and nitrogen donor atoms, which reflects the accumulation of electron density on these atoms and is consistent with their role in coordinating to the cobalt center. The most positive potentials are located on the peripheral hydrogen atoms and on the bromine and chlorine substituents, which represent the electron-poor regions of the molecule. The MEP analysis therefore shows that the donor atoms remain the primary nucleophilic sites even after coordination, while the halogenated periphery constitutes the electrophilic region. This information is useful for assessing the potential of the complex to interact with biological targets or to participate in charge-transfer processes.

HOMO–LUMO:

The frontier molecular orbital analysis (Fig. 7) was performed to evaluate the electronic structure and chemical reactivity of the proposed model. The calculated HOMO is mainly delocalized over the Schiff base ligands with a significant contribution from the cobalt center, whereas the LUMO is primarily localized on the ligand framework. The calculated HOMO and LUMO energies are −5.42 eV and −2.56 eV, respectively, giving a HOMO–LUMO energy gap of ΔE = 2.86 eV. This gap indicates a moderate electronic stability and suggests that the complex may be capable of participating in charge-transfer processes. The FMO analysis was therefore used to assess the electronic softness of the complex and to support the interpretation of its spectroscopic behavior.

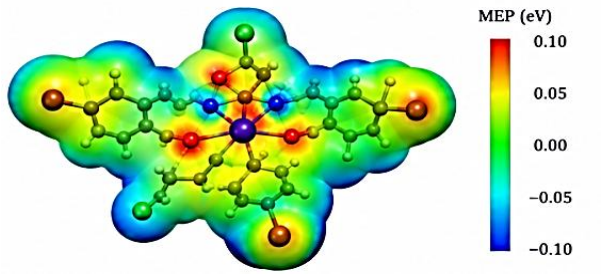


Figure 6. MEP of the cobalt complex.

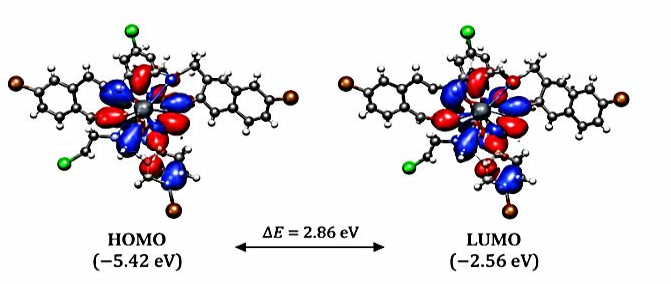


Figure 7. Homo-Lumo of the cobalt complex.

Source: Research Findings

3.6. NMR Analysis

The ^{13}C NMR spectrum in Fig. 8 is consistent with the formation of the cobalt Schiff base complex, as evidenced by the characteristic imine carbon signals appearing in the downfield region at 166.71 and 160.44 ppm. It should be emphasized that ^{13}C NMR spectroscopy provides information about the carbon framework of the ligand and supports the formation of the complex, but it does not by itself establish the oxidation state of the metal center. The Co(III) oxidation state was assumed in the computational model and requires independent experimental confirmation, for example by magnetic susceptibility or XPS measurements. The most diagnostic signals are the imine (C=N) carbons, which appear in the downfield region at 166.71 and 160.44 ppm. The presence of two distinct imine carbon signals is consistent with the two chemically inequivalent azomethine groups in the coordination sphere, which arises from the asymmetric arrangement of the three bidentate Schiff base ligands around the cobalt center. The downfield shift of these signals relative to the free ligand is attributed to the coordination of the imine nitrogen to the cobalt(III) center, which reduces the electron density at the azomethine carbon and thereby deshields it.

The aromatic region of the spectrum displays a cluster of signals between 135.49 and 109.81 ppm, corresponding to the aromatic carbons of the brominated salicylaldehyde moieties. The signals at the lower-field end of this region (approximately 135.49–130 ppm) are assigned to the quaternary aromatic carbons, including the carbon–oxygen (C–O) and carbon–bromine (C–Br) substituted carbons, while the signals in the range 120–109.81 ppm correspond to the protonated aromatic carbons. The presence of the C–Br substituted carbons in this region is consistent with the bromine substituents on the aromatic rings and provides further evidence for the integrity of the halogenated ligand framework.

In the aliphatic region, a prominent signal at 60.10 ppm is assigned to the methylene carbons adjacent to the coordinated nitrogen atoms (N–CH_2). This assignment is supported by the downfield position of this signal, which reflects the electron-withdrawing effect of the coordinated imine nitrogen. In addition, a signal at 45.39 ppm is attributed to the terminal chloromethyl carbons (CH_2–Cl) of the N-(2-chloroethyl) side chains. The presence of these two distinct aliphatic signals confirms that the chloroethyl groups remain intact and are not involved in coordination to the metal center. Importantly, the absence of signals corresponding to the free aldehyde carbonyl (typically observed at approximately 190–200 ppm) and to the unreacted primary amine indicates that the condensation reaction proceeded to completion and that the resulting complex is free of unreacted starting materials.

Furthermore, the number and distribution of the observed carbon signals are consistent with the proposed six-coordinate cobalt(III) complex bearing three bidentate Schiff base ligands, in agreement with the optimized geometry obtained from DFT calculations. Overall, the ^{13}C NMR data, in combination with the FT-IR, UV-Vis, and mass spectrometric results, support the formation of the target cobalt(III) Schiff base complex.

3.7. Photocatalysis experiment

Photocatalytic degradation experiments were performed to investigate the photocatalytic activity of the complex against methylene blue (MB) under solar light irradiation. The photocatalytic suspension was prepared by taking 4 mg of the prepared complex in 10 mL 10 mg L-1 MB water solution. To achieve adsorption–desorption equilibrium between dye molecules and complex, the solution was first kept in the dark for 30 min. Subsequently, the mixture was placed under sunlight irradiation to activate the photocatalytic process. At given time intervals, samples were withdrawn and centrifuged to remove the solid materials. The MB concentration was determined using UV–Vis spectrophotometry at the wavelength of 665 nm. Equation (1) was used to calculate the percentage degradation efficiency.

$$Percent\ degradation = (1 - Ct/C0) \times 100 \quad (1)$$

where C_t and C_0 represent the concentration of organic dye at time t and time 0, respectively;

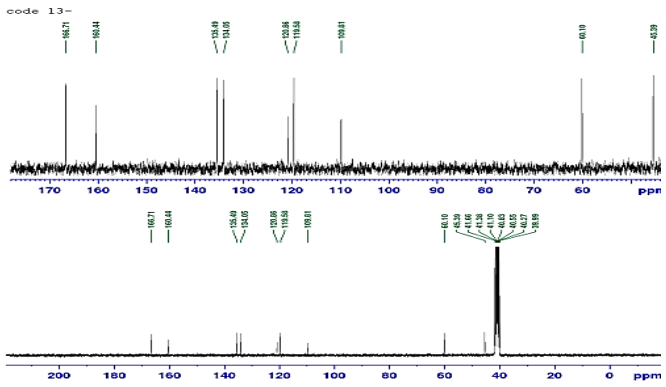


Figure 8. CNMR spectrum of the cobalt complex.

Source: Research Findings

Degradation of MB

The photocatalytic performance of the synthesized cobalt complex was investigated in the degradation of MB under solar light irradiation. As can be seen from Fig. 9a, the characteristic absorption peak intensity of MB at 665 nm gradually decreased with increasing irradiation time in the presence of the cobalt complex, indicating that the organic dye was degraded during the photocatalytic process. After 100 min of solar light irradiation, the degradation efficiency of the cobalt complex for MB was 69.48%. To determine the degradation rate of MB dye by the cobalt complex, a kinetic analysis was conducted using the Langmuir–Hinshelwood model, as shown in Eq. (2).

$$\ln\left(\frac{C_0}{C_t}\right) = kt \qquad (2)$$

where k (min^{-1}) and t (min) are degradation rate constant and irradiation time, respectively.

Fig. 9b shows the pseudo-first-order kinetic plot of MB degradation by the synthesized cobalt complex under solar light irradiation. The calculated rate constant (k) and correlation coefficients (R2) from the slope of the linear fit were found to be 0.0125, and 0.9803, respectively. The high value of R2 indicates that MB degradation follows pseudo-first order kinetics.

4. Conclusions

In this study, a cobalt complex with a Schiff base ligand bearing bromine substituents and chloroethyl groups was synthesized. FT-IR results provided evidence consistent with coordination of the ligand to the cobalt center. The UV-Vis spectrum revealed the electronic behavior of the ligand and weak bands in the visible region that may be cautiously attributed to d–d transitions of cobalt. The mass spectrum suggested the presence of halogen-containing species; however, definitive determination of the complex formula requires calculation of the theoretical isotope pattern and supplementary data. ICP analysis was performed, but no valid quantitative result was available at this stage. The ^{13}C NMR spectrum is consistent with the formation of the cobalt Schiff base complex. It should be noted that ^{13}C NMR spectroscopy does not establish the oxidation state of the metal center; the Co(III) oxidation state was assumed in the computational model and requires independent experimental confirmation.

Similar compounds have been investigated in previous studies for biological or catalytic applications [18–20]; however, evaluating such applications for the present complex requires dedicated experiments. Definitive determination of the metal oxidation state, molecular formula, and coordination geometry of the complex requires a set of supplementary data: elemental analysis (CHN) for composition, ICP for metal content, molar conductivity for electrolytic nature, magnetic susceptibility for electronic state. It should be noted that none of these methods alone is sufficient for definitive structure determination.

DFT calculations were performed to examine the proposed structure and electronic properties of the cobalt complex. The optimized geometry is consistent with a six-coordinate cobalt center in an approximately octahedral environment, coordinated by three imine nitrogen atoms and three oxygen donor atoms from three bidentate Schiff base ligands. The calculated vibrational frequencies reproduce the main features of the experimental FT-IR spectrum, including the imine C=N stretch and the Co–N and Co–O vibrations, supporting the proposed coordination environment. The FMO analysis gives a HOMO–LUMO gap of 2.86 eV, indicating moderate electronic stability and a possible tendency toward charge-transfer processes. The MEP map shows that the oxygen and nitrogen donor atoms are the most nucleophilic sites, while the halogenated periphery constitutes the electrophilic region. It should be emphasized that the Co(III) oxidation state was assumed in the computational model and is not independently confirmed by the DFT calculations. TD-DFT calculations were not performed because of the large size and heavy-atom composition of the complex and the associated computational cost; such calculations are recommended for future work to provide a more direct correlation with the experimental UV–Vis spectrum.

Author Contributions

Milad Mahjoobizadeh: Writing and Original Draft; Vahidreza Darugar: Investigation, Writing , Review and Editing; Satar Saberi: NMR Analysis; Somayeh Heydari: Photodegradation Analysis; Hasna Sadat Mirzaei: Data Curation.

Conflict of Interest

The authors, while observing publication ethics in the referencing, declare the absence of interest of conflict.

Acknowledgement

The authors gratefully acknowledge the support provided by University of Torbat-e Jam in conducting this research.

AI Use Statement

The authors retain full responsibility for the accuracy, originality, integrity, legality, and ethical compliance of all text, data, tables, figures, analyses, references, and conclusions, and have verified all AI-assisted outputs. Any fabrication, falsification, manipulation, plagiarism, copyright infringement, or other misuse of AI remains solely the responsibility of the authors and does not transfer or diminish their accountability for the published work.

References

[1] H. Schiff, *Justus Liebigs Annalen der Chemie*, 1864, **131(1)**, 118-119. https://doi.org/10.1002/jlac.18641310113

[2] T. T. Tidwell, *Angewandte Chemie International Edition*, 2008, **47(6)**, 1016-1020. https://doi.org/10.1002/anie.200702965

[3] R. H. Holm, G. W. Everett Jr, & A. Chakravorty, *Progress in Inorganic Chemistry*, 1966, **7**, 83-214. https://doi.org/10.1002/9780470166086.ch3

[4] P. A. Vigato, & S. Tamburini, *Coordination Chemistry Reviews*, 2004, **248(17-20)**, 1717-2128. https://doi.org/10.1016/j.ccr.2003.09.003

[5] M. Calligaris, & L. Randaccio, *Comprehensive Coordination Chemistry*, Pergamon, Oxford, 1987, ver 2, pp. 715–738.

[6] A. A. Khandar, S. A. Hosseini-Yazdi, & S. A. Zarei, *Inorganica chimica acta*, 2005, **358(11)**, 3211-3217. https://doi.org/10.1016/j.ica.2005.04.028

[7] K. C. Gupta, & A. K. Sutar, *Coordination Chemistry Reviews*, 2008, **252(12-14)**, 1420-1450. https://doi.org/10.1016/j.ccr.2007.09.005

[8] Z. H. Chohan, M. Arif, M. A. Akhtar, & C. T. Supuran, *Bioinorganic Chemistry and Applications*, 2006, **2006(1)**, 83131-83160. https://doi.org/10.1155/BCA/2006/83131

[9] N. Raman, R. Jeyamurugan, M. Subbulakshmi, R. Boominathan, & C. R. Yuvarajan, *Chemical Papers*, 2010, **64(3)**, 318-328. https://doi.org/10.2478/s11696-010-0003-0

[10] K. K. Naik, S. Selvaraj, & N. Naik, *Spectrochimica Acta Part A: Molecular and Biomolecular Spectroscopy*, 2014, **131**, 599-605. https://doi.org/10.1016/j.saa.2014.03.038

[11] B. G. Tweedy, *Plant extracts with metal ions as potential antimicrobial agents*, Phytopathology, 1964, ver. 55, pp. 910-914.

[12] N. Dharmaraj, P. Viswanathamurthi, & K. Natarajan, *Transition Metal Chemistry*, 2001, **26(1)**, 105-109. https://doi.org/10.1023/A:1007132408648

[13] N. N. Greenwood & A. Earnshaw. *Chemistry of the Elements*, Pergamon Press Ltd, 1984. https://doi.org/10.1016/C2013-0-03718-8

[14] F. A. Cotton, G. Wilkinson, C. A. Murillo, & M. Bochmann. *Advanced inorganic chemistry*, Willey, 1999.

[15] R. Golbedaghi, & S. Mohammadi, *Journal of Environmental Economics & Chemical Processes*, 2024, **1(1)**, 17-20. https://doi.org/10.22034/jeecp.2024.734998

[16] A. P. Lever, *Inorganic electronic spectroscopy*, Elsevier, 1984.

[17] R. Golbedaghi, A. Saberi, & N. Ilka, *Journal of Environmental Economics and Chemical Processes*, 2026, **3(3)**, 141-143. https://doi.org/10.22034/jeecp.2026.2089069.1025

[18] P. G. Cozzi, *Chemical Society Reviews*, 2004, **33(7)**, 410-421. https://doi.org/10.1039/b307853c

[19] M. J. Frisch. Et. Al, Gaussian 09, Revision D.01, Gaussian, Inc., Wallingford, CT, 2013.

[20] H. Schröder, A. Creon, & T. Schwabe, *Journal of chemical theory and computation*, 2015, **11(7)**, 3163-3170. https://doi.org/10.1021/acs.jctc.5b00400

[21] H. Mofid, M. R. Khosravi-Nikou, S. A. Razavi, & M. Mohammadian, *Applied Thermal Engineering*, 2024, **245**, 1-17. https://doi.org/10.1016/j.applthermaleng.2024.122810

[22] S. A. Razavi, & H. Motavali, *Journal of Industrial Engineering and Management Studies*, 2023, **10(2)**, 106-115. https://doi.org/10.22116/jiems.2023.399150.1516